

PAPER • OPEN ACCESS

Premelting as studied by positron annihilation and emission Mössbauer spectroscopies

To cite this article: S V Stepanov *et al* 2016 *J. Phys.: Conf. Ser.* **674** 012018

View the [article online](#) for updates and enhancements.

Related content

- [Feshbach projection operator approach to positron annihilation](#)
S d'A Sanchez, M A P Lima and M T do N Varella
- [Experimental investigation of refractory metals in the premelting region during fast heating](#)
V N Senchenko, R S Belikov and V S Popov
- [Calculation of gamma spectra for positron annihilation on molecules](#)
Dermot G Green, G F Gribakin, F Wang *et al.*

Recent citations

- [D-shell of iron atom of the amorphous FeCr15B15 alloy effective charge change during the crystallization](#)
Nikolay O. Khmelevsky *et al*



IOP | ebooks™

Bringing you innovative digital publishing with leading voices to create your essential collection of books in STEM research.

Start exploring the collection - download the first chapter of every title for free.

Premelting as studied by positron annihilation and emission Mössbauer spectroscopies

S V Stepanov^{1,2}, V M Byakov^{2,3}, D S Zvezhinskiy², G Duplâtre⁴, L Yu Dubov¹, P S Stepanov¹, Yu D Perfiliev⁵, L A Kulikov⁵

¹ National Research Nuclear University “MEPhI” (Moscow Engineering and Physical Institute), 115409, Moscow, Russia

² Institute of Theoretical and Experimental Physics, 117218, Moscow, Russia

³ D. Mendeleev University of Chemical Technology of Russia, 125047, Moscow, Russia

⁴ Institut Pluridisciplinaire Hubert Curien, CNRS/IN2P3, BP 28 67037 Strasbourg, France

⁵ Lomonosov Moscow State University, Chemical Department, Leninskie Gory, Moscow, Russia

stepanov@itep.ru

Abstract. We have estimated a local heating which takes place owing to the ionization energy losses at the terminal part of a fast positron track and at nano-vicinities of the ⁵⁷Fe Mössbauer nuclei in case of the emission Mössbauer spectroscopy. It is shown that in experiments close to the melting point one may expect local melting near the probe species.

1. Introduction

It is well known that positrons (e^+) as well as positronium atoms (Ps) are convenient probes of the local nanoscale structure in a condensed phase and the radiolytic processes occurring therein [1]. When a fast positron is injected into a molecular medium it loses most of its energy through ionizations. Within a few picoseconds this energy is locally converted into heat. Slightly below the melting point the heat is mainly transformed into a latent heat of fusion. As a result, a local melting of the terminal part of the e^+ track becomes possible. The radius of the molten region turns out to be several tens of Å. Consequently, the lifetime of the ortho-Ps atom produced therein, τ_3 , reaches its liquid-phase value at a temperature 2-3 degrees below the melting point. Apparently, this is due to the fact that the Ps atom is captured by the molten region of the e^+ track, where it forms a nanobubble (typical for liquids), while the bulk of the medium remains frozen [2]. Probably this Ps bubble may survive (as a local cavity), after cooling and solidification of this area.

The sensitivity of e^+ and Ps to the presence of structural defects opens a possibility to study the nature of phase transitions and, particularly, the accumulation of these defects at a stage of premelting, by detecting the annihilation radiation. We have carried out such a study in frozen alcohols and water [3]. Our preliminary estimations have shown that defects are accumulated in accordance with the Arrhenius law. The total energy spent for their formation approximately agrees with the latent heat of fusion.

In water, formation of the Ps bubble state in the premelted region is somewhat special. Because of the “negative” pressure within the molten “droplet” (due to the difference of densities between ice and liquid water), the Ps bubble becomes even larger than in bulky liquid water [4].



In this paper we discuss the local heating effect in the terminal part of the fast positron tracks as well as a similar effect which may take place in experiments on the emission Mössbauer spectroscopy (EMS) in frozen aqueous solutions. In the latter case local heating (and probably premelting) occur due to the emission and slowing down of the Auger electrons released by excited ^{57}Fe Mössbauer nuclei [5].

Further, fast radiation-chemical reactions in the Auger-blob (ion-electron recombination, electron localization and scavenging) determine the experimentally observable ratio of the yields of final chemically stable Fe^{3+} and Fe^{2+} . This ratio is important for adequate interpretation of the emission Mössbauer spectra. Reduction of the Fe^{3+} ion to the Fe^{2+} state occurs because of interaction with one of the blob quasifree electrons [6]. In [2] we have discussed the structure of a positron track. It was shown that, in its terminal part, positron ionization losses are most efficient. So there is the highest density of ion-electron pairs and chemically active radiolytic products (radicals), which are able to react with the positronium atom, formed therein. In accordance with radiation-chemical literature this part of the positron track is called the terminal blob. It consists of several tens of ion-electron pairs. Their spatial distribution can be approximated by the Gaussian function

$$c(r, t = 0) = N \frac{\exp(-r^2 / a^2)}{\pi^{3/2} a^3}, \quad (1)$$

where $a \approx 40 \text{ \AA}$ and $N \approx 30$ [2].

The positron blob formation energy, $W_{blob} \approx 500 \text{ eV}$, is released within the volume of the e^+ blob during a few femtoseconds. Then this energy is transformed into heat (over picoseconds), which leads to an increase of the local temperature of the blob.

A similar scenario occurs in the emission Mössbauer spectroscopy (EMS). In EMS experiments excited Mössbauer $^{57}\text{Fe}^*$ nuclei appear as a result of an electron capture by ^{57}Co nuclei (^{57}Co half-life is 272 days). Thus, the ^{57}Co nucleus transforms into a highly excited state, $^{57}\text{Fe}^*$ (136 keV), which during approximately 9 ns populates the low-lying Mössbauer nuclear level at 14.4 keV (its half-life is 98 ns).

Just after E-capture, the electronic structure of the Mössbauer iron ion corresponds to that of the initial $^{57}\text{Co}^{2+}$ ion, but with an electronic vacancy ("hole") usually on the K-shell. The excitation energy of this electronically excited iron ion may be estimated, knowing the wavelength-K α lines of the characteristic radiation of iron or cobalt, which are respectively equal to 0.194 nm and 0.179 nm (or 6.4 keV and 6.9 keV in energy units). This hole on the K-shell is filled with one of the electrons from the outer shells. This transition initiates the emission of the cascade of the Auger electrons with a total energy $W_{blob} \approx 6 \text{ keV}$. The emission of the Auger cascade leads to the formation of a multiply ionized iron ion, $^{57}\text{Fe}^{n+}$, where n may reach 8, averaging at 4-6.

However, this emission leads not only to formation of the multi-charged $^{57}\text{Fe}^{n+}$ ion, but also to formation of a cloud of many (200-300) ion-electron pairs (H_2O^+ , e^-) around this ion. Such a cloud is termed the Auger blob. Its radius is about $\sim 100 \text{ \AA}$ and its formation time is about 10^{-13} s [5]. Ionization slowing down of the Auger electrons initiates radiolytic processes in the nearest (nano)vicinity of the Mössbauer nucleus (ion). In [6, 7] EMC was applied for investigating these radiolytic processes in frozen aqueous solutions of different acids.

2. Simulations of the spatial distributions of the secondary electrons in the positron blob and the Auger blob

Modeling of the spatial distribution of the secondary electrons in tracks of the ionizing particles (in the positron blob and in the Auger blob) may be carried out with the help of the GEANT4 toolkit for the Monte Carlo simulation of the passage of particles through matter [geant4.cern.ch]. Application of its additional package, called DNA, allows to simulate the behavior of secondary electrons (i.e. to trace their trajectories) down to energies of about several eV.

To simulate the space distributions of secondary electrons in the Auger blob we have placed an isotropic (spherically symmetrical) source of fast electrons in the origin of coordinates. The initial

energies of the emitted electrons were chosen to be 0.5, 1 and 2 keV. GEANT4 takes into account scattering of the electrons and their energy loss processes, but does not take into account any process like ion-electron recombination, electron-electron Coulombic repulsion, trapping and so on. The resulting spatial distributions are shown in Figure 1. (in black, blue and brown). It is seen that at distances larger than 50, 100 and 200 nm the distributions abruptly cut off.

For obtaining the resulting spatial distribution of secondary electrons, we have to average these distributions over the initial energies of the Auger electrons. However, the respective distribution function is not known. So, for simplicity, when calculating the kinetics of local heating of the Auger blob, we approximated $c(r)$ by the Gaussian function (1) with the parameter a equal to 80-100 Å.

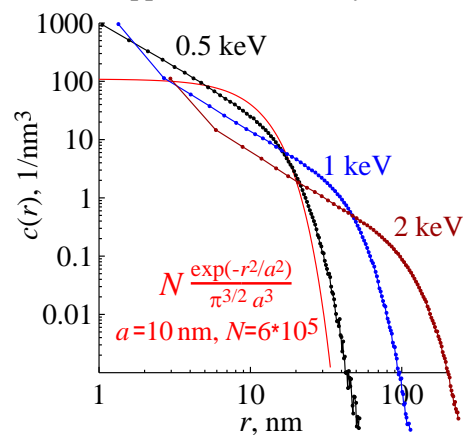


Figure 1. Results of the simulation of the radial distributions, $c(r)$, of the secondary electrons in the Auger blob by means of the GEANT4-DNA toolkit for three different initial energies of the emitted Auger electrons, 0.5, 1 and 2 keV. All distributions are normalized to the total number N of the secondary electrons: $\int c(r) 4\pi r^2 dr = N$. The total initial energy of all emitted Auger electrons in each energy group (0.5, 1, 2 keV) was about the same, 11 MeV. It was assumed that the excited iron ion is located at the origin of coordinates and isotropically emits Auger electrons. The red line is an approximation of $c(r)$ by the Gaussian function.

To obtain the distribution of the secondary electrons in the positron blob, we have used monidirectional (along z axis) emission of the positrons with the initial energy $W_{blob} \approx 500$ eV. The resulting axially symmetric distribution is shown in Figure 2.

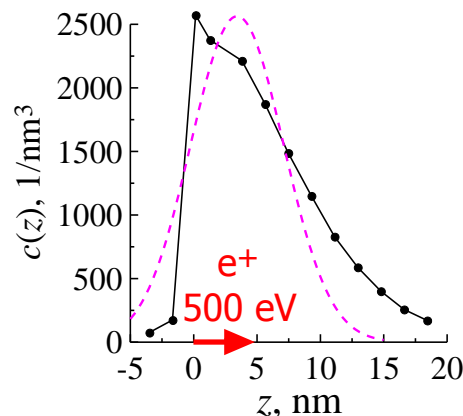


Figure 2. The axially symmetric distribution $c(z) = \int c(\mathbf{r}) dx dy$ of the secondary e^- in the positron blob, where e^+ loses its last 500 eV of energy. $\int c(z) dz = N$ is the total number of the secondary e^- . Positrons with energies $W_{blob} = 500$ eV are emitted from the point $z=0$ along z -axis. In this simulation the total number of all emitted positrons was about 1000. The dashed line is the approximation of $c(z)$ by the Gaussian distribution, shifted toward the direction of the initial momentum of the positron: $c(z) = N \exp(-(z-b)^2/a^2) / \pi^{1/2} a$, where $N \approx 24000$, $a = 5.2$ nm, $b = 3.4$ nm.

3. Effect of local heating in the positron blob and the Auger blob

Assuming that the distributions of secondary electrons in the positron blob and in the Auger blob directly correlate with the distributions of the released energy in space, we can estimate the effect of local heating initiated by the formation of the blobs. The distribution of the local temperature $T(r,t)$ can be obtained by solving the heat transfer equation [8]:

$$c_p \rho \partial T(r,t) / \partial t = \text{div} (\lambda \text{grad} T(r,t)) + q_+(r,t), \quad T(r,t=0) = T_{bulk}. \quad (4)$$

Here $T(r,t)$ is the local temperature, T_{bulk} is the temperature of the medium far from the blob, λ is the specific heat conductivity, ρ is the density, $c_p(T(r,t))$ is the heat capacity, which depends on the local temperature $T(r,t)$ of the medium (it is equal to the heat capacity of the solid phase $c_p^S(T)$, if $T(r,t) < T_m$, and to the heat capacity of the liquid, $c_p^L(T)$, if $T(r,t) > T_m$). Finally, $q_+(r,t)$ describes the heat source, i.e.

transformation of the ionization energy losses of the energized particles (positron, Auger electrons, secondary electrons) into heat:

$$q_+(r,t) = W_{blob} f(t,\tau) c(r,t=0)/N, \tag{5}$$

where W_{blob} is the blob formation energy, the function $f(t,\tau) = \exp[-(t-3 \text{ ps})^2/2\tau^2]/(2\pi)^{1/2}\tau$, $\tau = 1 \text{ ps}$ describes the transformation of the energy of primary and secondary particles (into heat) in time and $c(r,t=0)/N$ represents the spatial distribution of the released energy.

To utilize Eq. 4 at temperatures close to the melting point T_m of the frozen phase, one may use the following approach [9]. At temperatures slightly below T_m we add to the heat capacity $c_p^S(T)$ of the solid phase a quasi-singular contribution, which takes into account absorption of the enthalpy of fusion. In view of a numerical solution of the heat transfer equation we approximate this contribution by a narrow Gaussian function with the width $\Delta T = 0.25 \text{ }^\circ\text{C}$ centered at $T_m - 3\Delta T$ (slightly below T_m), namely:

$$c_p(T(r,t)) \rightarrow c_p(T(r,t)) + q_m \exp[-(T(r,t) - T_m - 3\Delta T)^2/2\Delta T^2] / (2\pi)^{1/2}\Delta T. \tag{6}$$

An integral over temperature from this additional contribution (the last term in Eq. 6) is equal to the specific latent heat of melting (or the enthalpy of fusion), which is q_m :

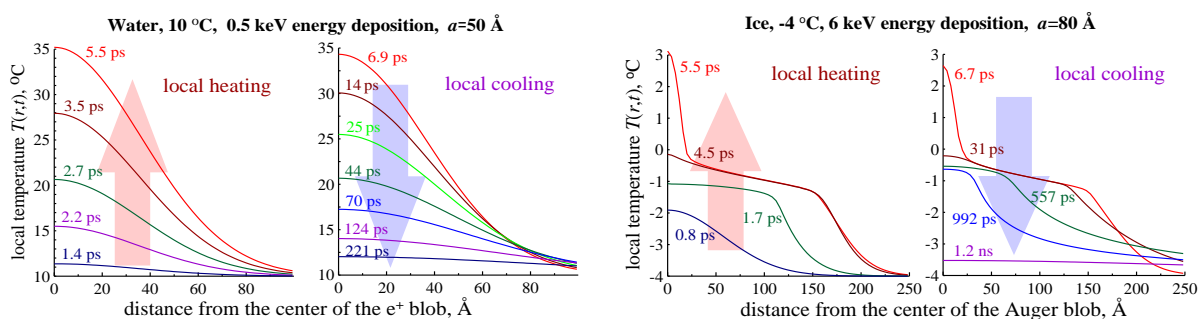
$$q_m \int dT \exp[-(T(r,t) - T_m - 3\Delta T)^2/2\Delta T^2] / (2\pi)^{1/2}\Delta T = q_m. \tag{7}$$

For description of the temperature dependences of the thermal conductivity $\lambda(T)$ and density $\rho(T)$ close to the melting point we have used slightly smoothed (within the interval $\sim\Delta T$ for convenience of the numerical calculations) step-like approximations, which match values of λ and ρ in the solid and liquid phases: $\lambda(T(r,t) < T_m) = \lambda^S$, $\lambda(T(r,t) > T_m) = \lambda^L$ and $\rho(T(r,t) < T_m) = \rho^S$, $\rho(T(r,t) > T_m) = \rho^L$.

In the calculations we used the following parameters [10, 11]:

	T_m , [K]	λ^S ; λ^L , [W/m/K]	q_m , [J/g]	c_p^S ; c_p^L , [J/g/K]	ρ^S ; ρ^L , [g/cm ³]	M, [g]
ice / water	273.15	2.38 ; 0.56	334	2.06; 4.18	0.92 ; 1.00	18

In numerical solution of Equation 4, were designed kinetics of heating / cooling of the blob as a liquid or in a frozen aqueous medium. For the e+ blob we used $W_{blob} = 500 \text{ eV}$ and $a = 40\text{-}50 \text{ \AA}$, and for the Auger blob $W_{blob} = 6 \text{ keV}$ and $a = 80\text{-}100 \text{ \AA}$. The calculation results are presented in Figure 3.



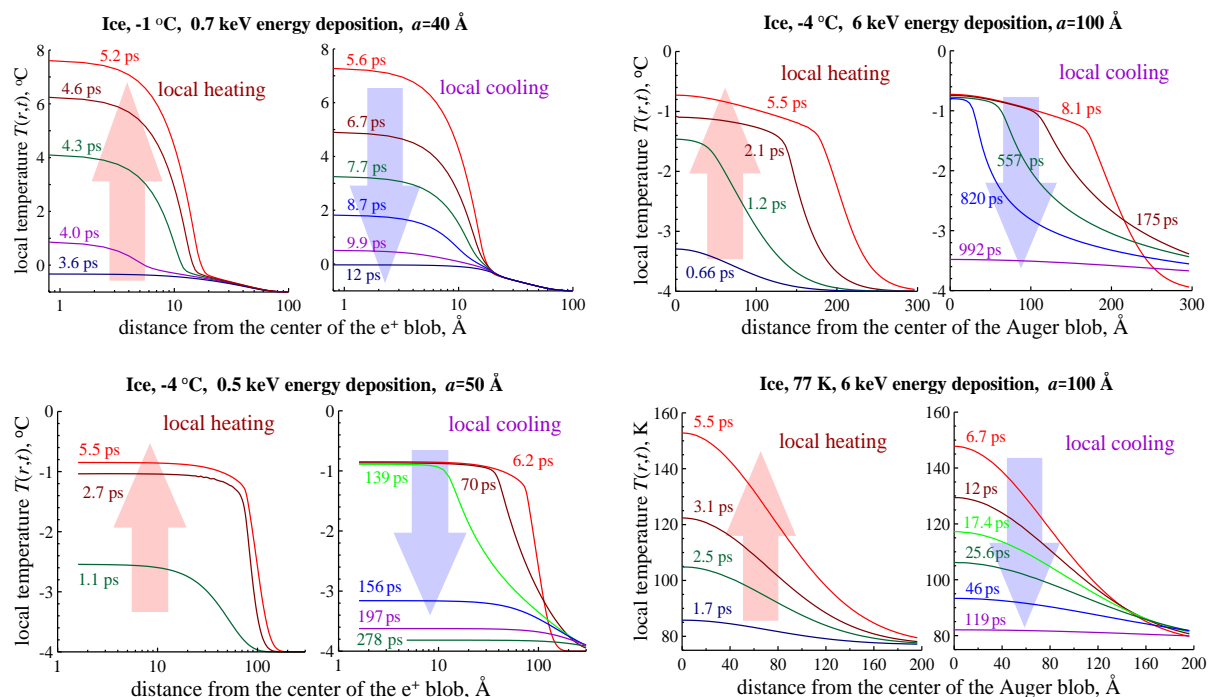


Figure 3. Temperature profiles of heating/cooling of the positron blob and the Auger blob.

4. Conclusion

It is known that during irradiation at low temperatures many intermediate radiolysis products become stabilized. Blob electrons are captured by structural traps, thereby forming trapped electrons, e_{tr}^- . At elevated temperatures, different types of motion become possible and trapped electrons may recombine with counterions and radicals, which results in luminescence (thermoluminescence). It is known that the maximum of thermoluminescence for ice irradiated by gamma-rays at 77 K is observed at $T \approx 110$ -113 K [12]. The above calculations show that such an increase of local temperature in the Auger blob is quite possible. It may increase the reactivity of e_{tr}^- with respect to intrablob radiolytic products and $^{57}\text{Fe}^{3+}$ ions as well. Moreover in EMS experiments at T slightly below T_m , melting of the central part of the Auger blob is possible (for several tens of picoseconds) which may lead to the complete disappearance of the Mössbauer effect.

In the positron blob melting is also possible. We have to note that water is somewhat an inconvenient medium for studying premelting: the thermal conductivity of ice is 10 times larger than that of most molecular media, and the hidden heat of melting is also several times as large. Nevertheless, premelting was observed in ice [4]. So other molecular media could prove to be more convenient for studying premelting effect.

References

- [1] Jean Y C, Mallon P E, Schrader D M (Eds.) 2003 *Positron and Positronium Chemistry* (World Scientific, Singapore)
- [2] Stepanov S V, Byakov V M, Zvezhinskiy D S, Duplâtre G, Nurmukhametov R R, Stepanov P S 2012 *Adv. Phys. Chem.* **2012** 431962
- [3] Zvezhinskiy D S, Stepanov S V, Byakov V M, Zgardzinska B 2013 *Mat. Sci. Forum* **733** 15
- [4] Zgardzinska B, Goworek T 2014 *Phys. Lett. A* **378**, 915
- [5] Byakov V M, Perfil'ev Yu D, Kulikov L A, Stepanov S V 2009 *Moscow University Chemistry Bulletin* **64** 259
- [6] Byakov V M, Kulikov L A, Perfil'ev Yu D, Stepanov S V 2005 *Acta Phys. Pol. A* **107** 792

- [7] Stepanov S V, Perfil'ev Yu D, Byakov V M, Kulikov L A 2014 *Acta Phys. Pol. A* **125** 843
- [8] Muhieddine M, Canot E, March R 2009 *Int. J. of Fin.* **6** 1
- [9] Bonacina C, Comini G, Fasano A, Primicerio M 1973 *Int. J. Heat Mass Tran.* **16** 1825
- [10] Yaws C 1999 *Lange's Handbook Of Chemistry*, 15-th Edition (McGRAW-HILL, INC)
- [11] The 84th Edition of the Handbook of Chemistry and Physics. CRC Press LLC, 2004
- [12] Pikaev A K *Modern radiation chemistry. Solid state and polymers. Applied aspects* (Moscow, Nauka, 1987)